Journal of Hazardous Materials 213–214 (2012) 71–82

Contents lists available at SciVerse ScienceDirect

Journal of Hazardous Materials

journal homepage: www.elsevier.com/locate/jhazmat

A novel silica alumina-based backfill material composed of coal refuse and fly ash

Yuan Yao[a,c], Henghu Sun[a,b,*]

[a] Pacific Resources Research Center, University of the Pacific, Stockton, CA 95211, USA
[b] School of Engineering and Computer Science, University of the Pacific, Stockton, CA 95211, USA
[c] Pharmaceutical and Chemical Science Program, University of the Pacific, Stockton, CA 95211, USA

ARTICLE INFO

Article history:
Received 10 June 2011
Received in revised form
15 December 2011
Accepted 17 January 2012
Available online 24 January 2012

Keywords:
Backfill
Coal refuse
Fly ash
Performance
Microanalysis

ABSTRACT

In this paper, a systematic study was conducted to investigate a novel silica alumina-based backfill material composed of coal refuse and fly ash. The coal refuse and fly ash had different properties under various thermal activation temperatures (20 °C, 150 °C, 350 °C, 550 °C, 750 °C and 950 °C). It is known that a thermal activation temperature ranging from 20 °C to 950 °C significantly increases the flowability and pozzolanic properties of the coal refuse; however, the flowability of fly ash decreases when the activation temperature is higher than 550 °C because of a severe agglomeration phenomenon on its surface. An optimal design for this backfill material was determined to include an activated portion composed of 5% coal refuse at 750 °C and 15% fly ash at 20 °C. This combination yields the best performance with excellent flowability, a high compressive strength and a low bleeding rate. The microanalysis results corresponded well with the performance tests at different activation conditions. In the coal refuse, kaolinite peaks began to decrease because of their transformation into metakaolin at 550 °C. Chlorite peaks disappeared at 750 °C. Muscovite peaks decreased at 750 °C and disappeared at 950 °C. During this process, muscovite $2M_1$ gradually dehydroxylated to muscovite HT. Furthermore, this paper examined the environmental acceptance and economic feasibility of this technology and found that this silica alumina-based backfill material composed of coal refuse and fly ash not only meets EPA requirements but also has several advantages in industry feasibility when compared with hydraulic backfill, rock backfill and paste backfill.

Published by Elsevier B.V.

1. Introduction

The coal industry has been the fastest-growing fuel industry over the last decade because of its role as the primary fuel used for electricity generation [1]. Coal refuse is one of the largest forms of waste from the coal mining industry and is generally defined as a low BTU-value material based on the minimum ash content combined with the maximum heating value [2]. It is estimated that coal mines in the US generate 109 million metric tons (120 million short tons) of coal refuse from 600 coal preparation plants in 21 coal-producing states annually [3]. Presently, two major methods are applied for the utilization of coal refuse: combustion use and non-combustion use. However, the utilization efficiency of coal refuse remains low [2,3].

Backfill refers to any waste material that is placed in voids mined underground for the purpose of either disposal or performing engineering functions [4]. The backfill industry is particularly interested in technologies that reduce the costs associated with backfilling large open stopes [5]. Previous studies on backfill using industrial waste have been conducted in the last decade, including studies on fly ash, blast furnace slag and flue gas desulfurization gypsum (FGD gypsum) [6,7], and reports on developed backfill materials have demonstrated their excellent workability and good mechanical properties [8,9]. Therefore, backfill material acts as a suitable solution to current industrial solid waste challenges [10,11]. However, there have been few studies on backfill material based on coal refuse, although some research has been conducted on the cementitious material composed of thermal activated coal refuse as pozzolanic material. Zhang et al. have successfully recycled red mud and coal refuse into cementitious material by thermal activation at 600 °C [12,13], and Zhang has demonstrated that coal refuse contains good pozzolanic properties after thermal activation [14–16]. In this paper, a systematic study was conducted on a novel, high-performance, silica alumina-based backfill material, which was designed by taking advantage of the pozzolanic property of thermal activated coal refuse and the good flowability of fly ash. Furthermore, a detailed microanalysis is performed to illustrate the mechanism of coal refuse thermal activation and environmental leaching. The results proved the environmental acceptance of this new backfill material.

* Corresponding author at: 3601 Pacific Ave, University of the Pacific, Stockton, CA 95211, USA. Tel.: +1 209 946 2767; fax: +1 209 946 2077.
E-mail address: hsun@pacific.edu (H. Sun).

0304-3894/$ – see front matter. Published by Elsevier B.V.
doi:10.1016/j.jhazmat.2012.01.059

Table 1
Chemical analysis of the coal refuse.

LOD 105 °C, % (w/w)	Ash 750 °C, % (w/w)	Volatile matter, % (w/w)	Fixed carbon, % (w/w)	Total carbon, % (w/w)	Organic carbon, % (w/w)	Total sulfate, % (w/w)	Total nitrogen, % (w/w)	HHV BTU/lb
2.21	90.09	7.50	<1	3.43	3.05	0.041	0.10	342

2. Materials and experimental procedure

2.1. Materials

The raw material used in this experiment included coal refuse, fly ash, cement, blast furnace slag and FGD gypsum. The coal refuse was generated by a mining operation situated within the Central Appalachian Coal Basin in southwest Virginia, eastern Kentucky and southern West Virginia. The coal seams located near these operation sites were deposited during the Pennsylvania period and are located in the Pottsville Group from Pocahontas through the lower portions of the Allegheny formation. The fly ash is a typical combustion byproduct from the coal power plant in Tennessee, which was responsible for a catastrophic spill in 2008. According to the American Society for Testing and Materials (ASTM) C618, the fly ash used in this test should be designated as Class F [17]. The FGD gypsum was from Wisconsin, and the cement applied in the experiment was US type I/II, which has sufficient cohesion and strength to form ettringite in the backfill material.

2.2. Chemical, mineral and physical analyses

The chemical analysis was performed using an X-ray fluorescence (XRF-1700) analyzer, and the mineral composition was detected by X-ray diffraction (XRD) with the Rigaku Ultimate. The particle size pattern was measured using sieves and a laser particle distribution analyzer (Mastersizer 2000).

2.3. Thermal activation

Thermal activated oxidation occurred as the raw material (coal refuse or fly ash, respectively) reacted with oxygen in air. Thermal activation experiments were controlled at different temperatures (150 °C, 350 °C, 550 °C, 750 °C and 950 °C) inside a furnace (Lindberg Blue M, Thermo Scientific) for 45 min per experiment.

2.4. Flowability test

According to previous research and an ACI 229 report, ASTM D6103 was used to evaluate the consistency of the controlled low strength material [18]. An open-ended flow cylinder 6 in. (150 mm) in length with a 3 in. (76 mm) internal diameter was used to test the flowability by measuring the spread diameter when the fresh slurry was released from the cylinder onto a flat surface. It is important to immediately measure the largest resulting spread diameter of the backfill material. Then take two measurements of the spread diameter perpendicular to each other. The measurements are to be made along diameters which are perpendicular to one another [19].

2.5. Compressive strength test

For the compressive strength test, 50 mm × 50 mm × 50 mm cube specimens were cast for each mixture as described in previous research [9]. The compression tests were performed on six specimens of various ages (1, 3, 7, 28, 56 and 90 days). This material was carefully demolded for 24 h after it was cast because of its low and late increase in strength. However, before this process, the samples should be placed in sealed plastic bags to retain humidity. Each recipe had 12 replicates in these experiments.

2.6. Bleeding test

A high bleeding rate is often observed in fly ash-based cementitious material because of the spherical shape of the fly ash particle. In this test, as described in ASTM C232, the water bleeding rate was measured according to the amount of water accumulated at different time intervals on the sample surface of an approximately 14 l cylindrical container with an inside diameter of 255 ± 5 mm and a height of 280 ± 5 mm [20].

2.7. Microanalysis

In this experiment, X-ray diffraction (XRD) analysis was conducted using a Rigaku Ultimate, with CuKα radiation, a voltage of 40 kV, a current of 40 mA and a 2θ scan ranging between 5° and 60°. The Nicolet Impact 400 Fourier transform infrared (FTIR) spectroscopy was used to record the spectra with a Nicolet sample processor using KBr-pellets. The microstructures were observed by a Philips XL30 FEG Scanning Electron Microscope (SEM) with energy-dispersive X-ray microanalyses. The thermal gravimetric analysis (TGA) of the coal refuse was conducted between room temperature and 1000 °C at 20 °C/min.

2.8. Toxicity characteristic leaching procedure (TCLP)

The contaminant leaching tests for the raw material and 180 day backfill sample were conducted according to the EPA-TCLP1311-92 procedure. The concentrations of heavy metals were analyzed using Vista-PRO Varian ICP-OES.

3. Results and discussion

3.1. Characterization of raw material

Tables 1 and 2 summarize the chemical composition and physical properties of the raw materials. The total carbon in the coal refuse used in the experiment was 3.43%, and the higher heating value (HHV) was 342 BTU/lb. These results indicated that the coal refuse was not suitable for direct combustion use. The loss on drying (LOD) was 2.21% after being exposed to air at 105 °C for 1 h. The samples were stage ashed to 750 °C and held at that temperature

Table 2
Chemical composition and physical properties of the raw materials.

	Coal refuse	Fly ash	Slag	Gypsum	Cement
SiO_2 (%)	48.77	49.54	36.59	0.76	13.71
Al_2O_3 (%)	14.54	19.11	13.17	0.19	2.66
Fe_2O_3 (%)	11.12	14.79	0.98	0.17	3.27
CaO (%)	4.34	6.23	35.53	42.29	63.39
MgO (%)	1.68	0.42	7.58	0.71	1.23
SO_3 (%)	0.43	0.34	2.03	53.75	2.19
Loss on ignition (%)	9.91	2.43	2.78	1.98	2.6
Specific gravity (t/m^3)	2.69	2.38	2.98	2.91	3.18
Specific surface area (m^2/kg)	564	551	677	579	372

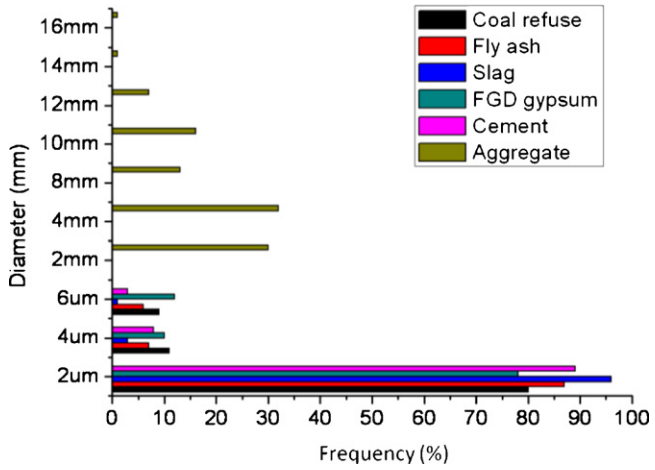

Fig. 1. Particle size distribution of the raw materials.

for 8 h to determine the ash percentage, which was 90.09%. The percentages of total sulfate and total nitrogen in the coal refuse were also very low.

According to ASTM C618, the fly ash used in this experiment was a class F fly ash because the CaO content was 6.23% [17]. According to the XRD analysis, the blast furnace slag was a glass-based material with a complicated, strong hump in the 15–45° 2θ region on the XRD result, indicating that the predominant phase was amorphous. The major mineral component of the coal refuse was quartz, followed by chloride, muscovite, kaolinite, hematite and calcite. The fly ash exhibited very clear principal peaks of quartz, mullite, hematite and calcite.

The raw coal refuse used in the experiments was an irregular, rock-like stone with a large size range from 1 mm to 30 cm. In this experiment, the raw coal refuse was divided into two categories: coarse coal refuse as aggregate and coal refuse after milling as pozzolanic material with a specific surface area of 564 m^2/kg when measured using the Blaine method. As was the case for the raw fly ash, the particle size was smaller than that of the raw coal refuse, and the fly ash after milling had a specific area of 551 m^2/kg. The industrial commercial slag, cement and FGD gypsum were in a fine powder state, with high Blaine values. The aggregate was a mixture of different size of coarse coal refuse. Fig. 1 illustrates the particle distribution of the raw materials. Except for the coal refuse aggregate, all of the raw material fell into the range of 1–6 μm, and more than 80% of the particles were less than 2 μm. Most of the coal refuse aggregate ranged from 1 mm to 16 mm in diameter, with the highest frequency distribution being 1–4 mm; however, there were still some large particle size distributions in the aggregate, such as 7% at 12 mm, 1% at 14 mm and 1% at 16 mm. All of the raw material was below 19 mm, which meets the ASTM D6103 standard [19].

Table 3
Composition of Backfill Material Group A.

	Cement	Slag	FGD gypsum	Activated material		Aggregate
				Coal refuse	Fly ash	
A1% (w/w)	1	1	1	20	0	77
A2% (w/w)	1	1	1	0	20	77

3.2. Flowability test for the coal refuse and fly ash

Fig. 2 clearly shows that the fly ash has better flowability than the coal refuse when they have the same water/solid (W/S) ratio. For example, when the W/S was 0.4, the spread diameter for the 20 °C coal refuse was only 94 mm, whereas that of the 20 °C fly ash was 265 mm. This result is due to the spherical shape of the fly ash ball, which behaves as a non-Newtonian fluid with a low permeability coefficient that reduces pipeline wear (the cylinder wall in this experiment). On the other hand, the coal refuse after milling is an irregular particle, which is more abrasive to the cylinder wall. However, it is interesting to note that the thermal activation of the coal refuse increased its flowability; however, the thermal activation did not notably improve the flowability of the fly ash. Furthermore, when the temperature was increased to more than 750 °C, the activated fly ash (750–950 °C) powder showed an agglomeration phenomenon that was more intense than that of the activated coal refuse (750–950 °C). Therefore, there was a decreasing tendency in the flowability at temperatures between 550 °C and 950 °C for the fly ash. However, the total flowability of the coal refuse increased at temperatures of 20–950 °C.

3.3. Performance of the backfill material

Generally, the backfill material contained different categories of raw material, including water, cementitious material, aggregates and others. The variation in the composition of the backfill material significantly influenced its performance. To obtain the performance characteristics of the backfill material, it is necessary to evaluate the flowability of the fresh backfill slurry and the compressive strength of the hardened body at different pulp densities (the amount of solid material of the total backfill material). Table 3 and Fig. 3

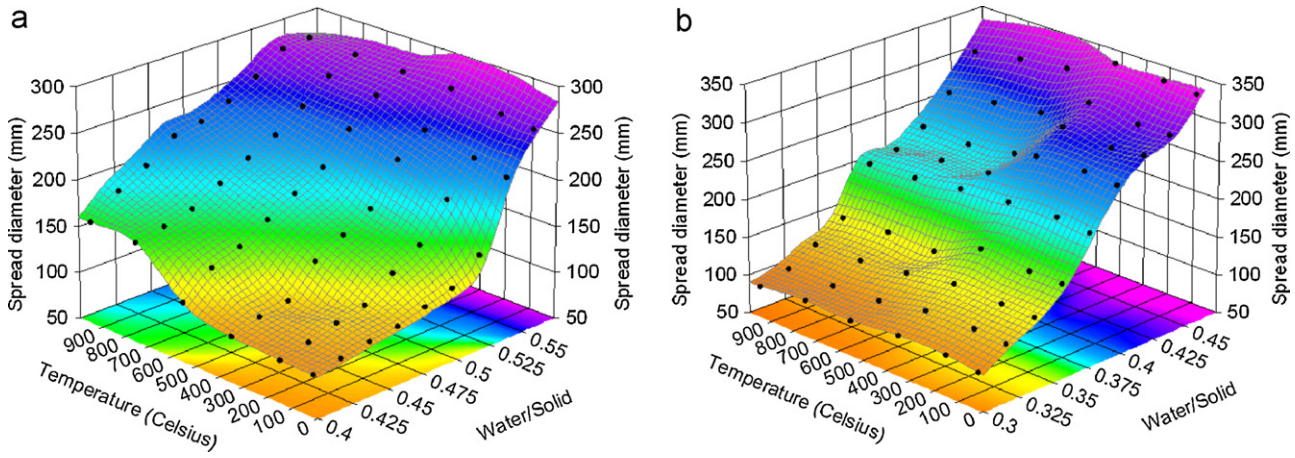

Fig. 2. Flowability test of coal refuse and fly ash: (a) coal refuse and (b) fly ash.

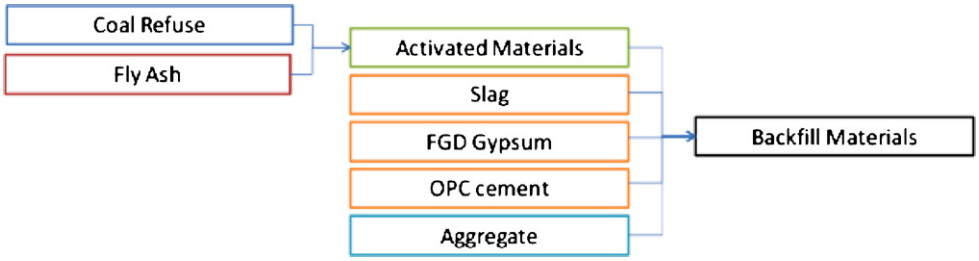

Fig. 3. Scheme chart of the backfill material design.

present the composition and design scheme of the tested backfill material in this experiment. Generally, the solid part of this backfill material is divided into three categories: cementitious material (cement + slag + FGD gypsum), activated material (coal refuse or fly ash) and aggregates.

Fig. 4(a) and (b) depicts the flowability of the backfill material at different pulp densities. The fly ash-based backfill material had better flowability than the coal refuse-based backfill material at the same pulp density. For example, when the pulp density was 70%, the spread of the 20 °C coal refuse-based backfill material was 201 mm, whereas that of the 20 °C fly ash-based backfill material was 301 mm. The various contents of the thermal-activated material showed different flowability patterns, and thermal activation from 20 °C to 950 °C significantly increased the flowability of the coal refuse-based backfill material. However, the flowability of the fly ash-based backfill material began to decrease when the activation temperature exceeded 550 °C.

Unconfined compressive strength is another important factor to evaluate the performance of backfill material. Fig. 4(c) and (d) shows the compressive strength measured at six different curing times (1, 3, 7, 28, 56 and 90 days) at a pulp density of 70%. It was found that the activated coal refuse-based backfill material had a higher unconfined compressive strength than that of the fly ash-based backfill material, indicating that the activated coal refuse has better pozzolanic properties than the activated fly ash. Thermal activation from 20 °C to 950 °C increased the pozzolanic property of the activated coal refuse and was better than the pozzolanic property of the activated fly ash at the same activation temperature, especially in the 90 day sample. For instance, the 750 °C coal refuse-based backfill material had an unconfined compressive strength of

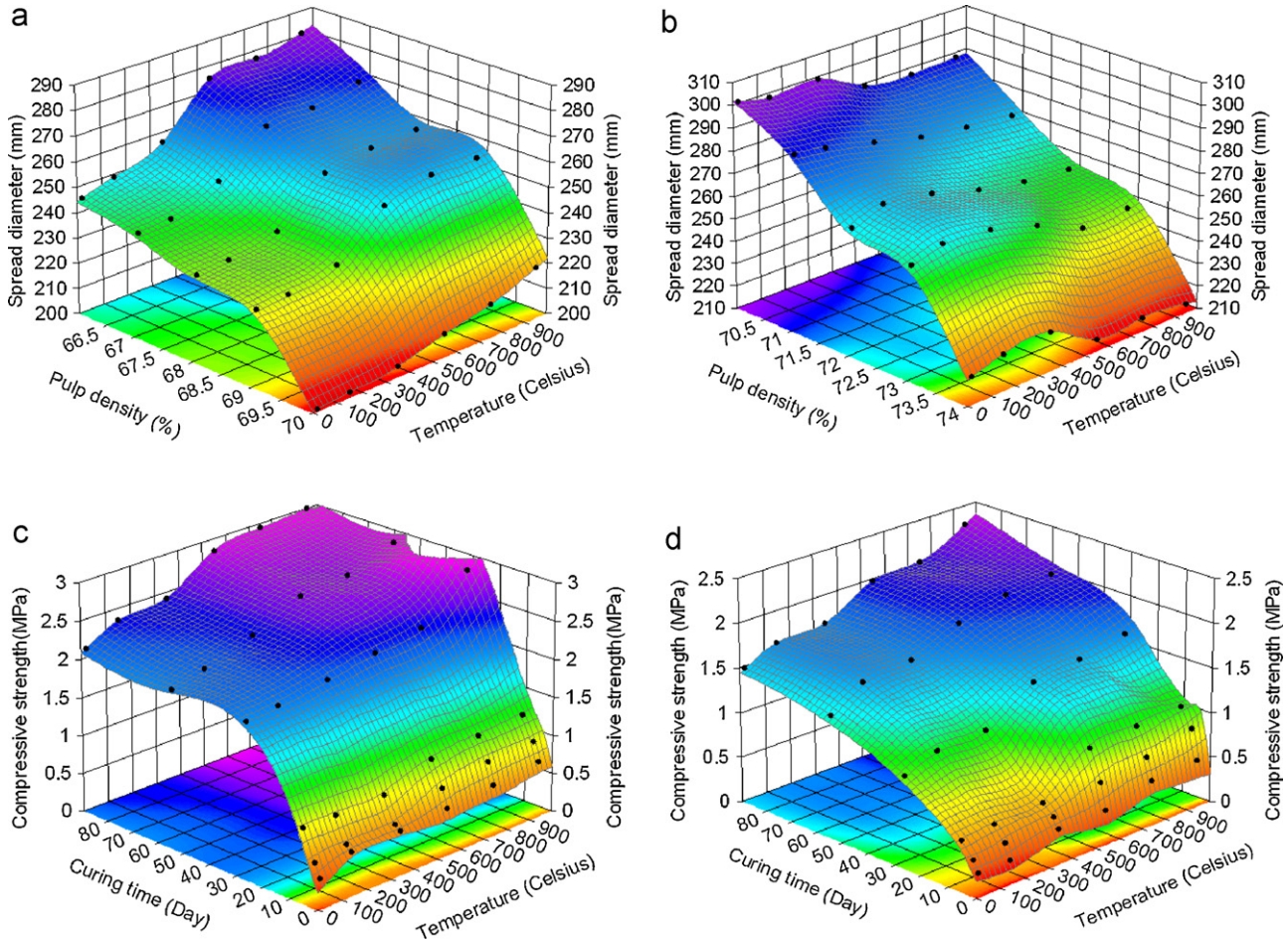

Fig. 4. Performance of the backfill material. (a) Flowability of the coal refuse-based backfill material, (b) flowability of fly ash-based backfill material, (c) compressive strength of the coal refuse-based backfill material and (d) compressive strength of the coal refuse-based backfill material.

Table 4
Composition of Backfill Material Group B.

	Cement	Slag	FGD gypsum	Activated material		Aggregate
				750 °C coal refuse	20 °C fly ash	
B1% (w/w)	1	1	1	20	0	77
B2% (w/w)	1	1	1	15	5	77
B3% (w/w)	1	1	1	10	10	77
B4% (w/w)	1	1	1	5	15	77
B5% (w/w)	1	1	1	0	20	77

2.94 MPa after 90 days of curing, which was not significantly different from the 2.98 MPa found in the 950 °C coal refuse-based backfill material. The 750 °C fly ash-based backfill material had an unconfined compressive strength of 2.02 MPa at 90 days, and the 950 °C fly ash-based backfill material reached 2.31 MPa.

3.4. Optimal design of backfill material

As mentioned above, thermal activation improved the pozzolanic properties and the flowability of the coal refuse; however, this method was not successful for the fly ash and instead resulted in decreased flowability caused by fly ash agglomeration beyond 550 °C. Considering the economic and environmental factors, the optimal design was found when combining the advantages of the 750 °C coal refuse and 20 °C fly ash because the fly ash slurry had much higher flowability than the coal refuse slurry below 550 °C. Table 4 lists the composition of Backfill Material Group B (B1–B5), which can be used to determine the optimal design for the backfill material with a mixture of 750 °C coal refuse and 20 °C fly ash.

Fig. 5 illustrates the flowability tests of B1–B5. These tests indicated that increasing the content of the 20 °C fly ash greatly improved the flowability of the fresh slurry. According to backfill work experience, ACI regulations and previous research, a range between 200 mm and 300 mm is acceptable for mining backfill applications [21]. B4 (5% 750 °C coal refuse + 15% 20 °C fly ash) is an optimal design for flowability because most of the spread fell within 200–300 mm when the pulp density was shifted from 70% to 75%. Although B5 (0% 750 °C coal refuse + 20% 20 °C fly ash) had slightly better flowability than B4, B5 is not a good choice when bleeding and compressive strength are considered. High content fly ash-based backfill material has a bleeding problem because

Table 5
Bleeding rates of B1–B5.

	B1	B2	B3	B4	B5
Bleeding rate (%)	2.45	2.87	3.01	3.29	6.07

of the spherical ball shape of the fly ash [10]. The 5% coal refuse has better water absorption ability when compared with the same amount of fly ash. Table 5 illustrates the bleeding rate of B1–B5 at a pulp density of 73%. The increased amount of coal refuse reduced the bleeding rate. The bleeding rate difference between B4 (3.29%) and B5 (6.07%) was significant. Fig. 6 shows that the compressive strength of B4 at a pulp density of 73% met the target compressive strength requirements for 28 days (1 MPa) for the backfill industry [6]; the 28 day strength was 1.4 MPa, and the 90 day strength was 2.7 MPa.

3.5. Microanalysis results

3.5.1. TGA result

To set up an optimal thermal activation condition for the coal refuse, a TGA was conducted from 25 °C to 1000 °C, and the results are shown in Fig. 7. The weight loss was approximately 1.2% at a temperature range of 25–450 °C. Comparatively, the weight loss was approximately 8.6% at a temperature range of 450–900 °C. When the temperature was above 900 °C, the weight loss was less than 0.1%. The chemical bonding water, which was defined as the mass due to decomposition between the boiling temperature and 1000 °C accounts for a portion of mass loss after 100 °C. In addition, the major mass loss from 500 °C to 700 °C was associated with the decomposition of minerals. For example, the decompositions of calcite and kaolinite are two important processes during this thermal activation stage, and the reactions can be generally expressed as the following [22,23]:

At 600–780 °C,

$$\underset{\text{(calcite)}}{CaCO_3} \rightarrow \underset{\text{(lime)}}{CaO} + CO_2$$

At 500–700 °C,

$$\underset{\text{(kaolinite)}}{Al_2O_3 \cdot 2SiO_2 \cdot 2H_2O} \rightarrow \underset{\text{(metakaolinite)}}{Al_2O_3 \cdot 2SiO_2} + 2H_2O$$

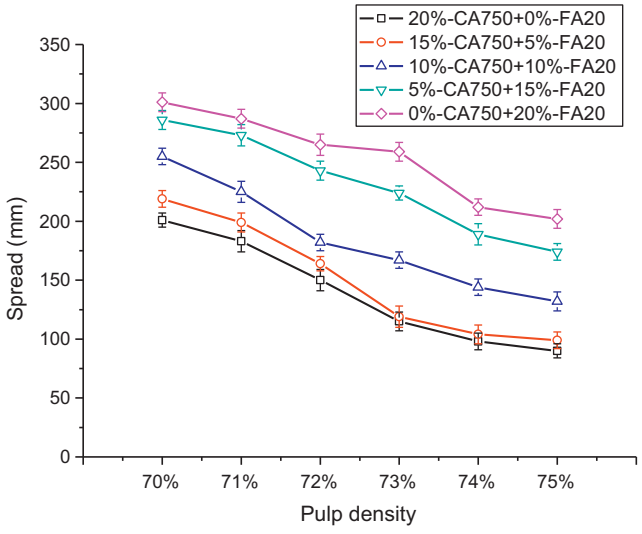

Fig. 5. Flowability test of Backfill Material Group B.

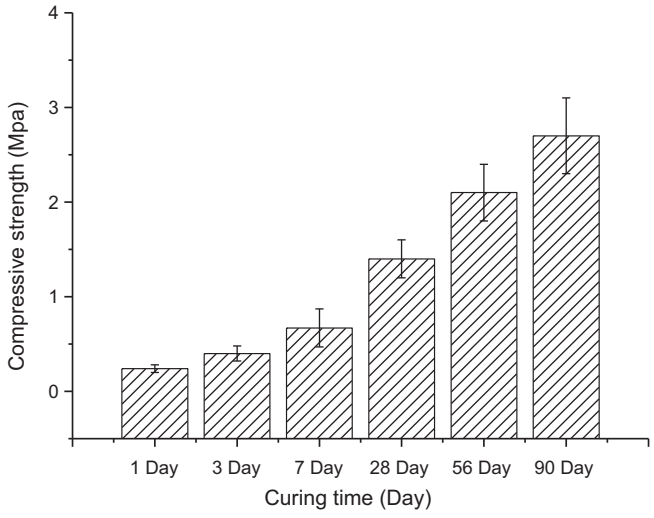

Fig. 6. Compressive strength test of Backfill Material Group B4.

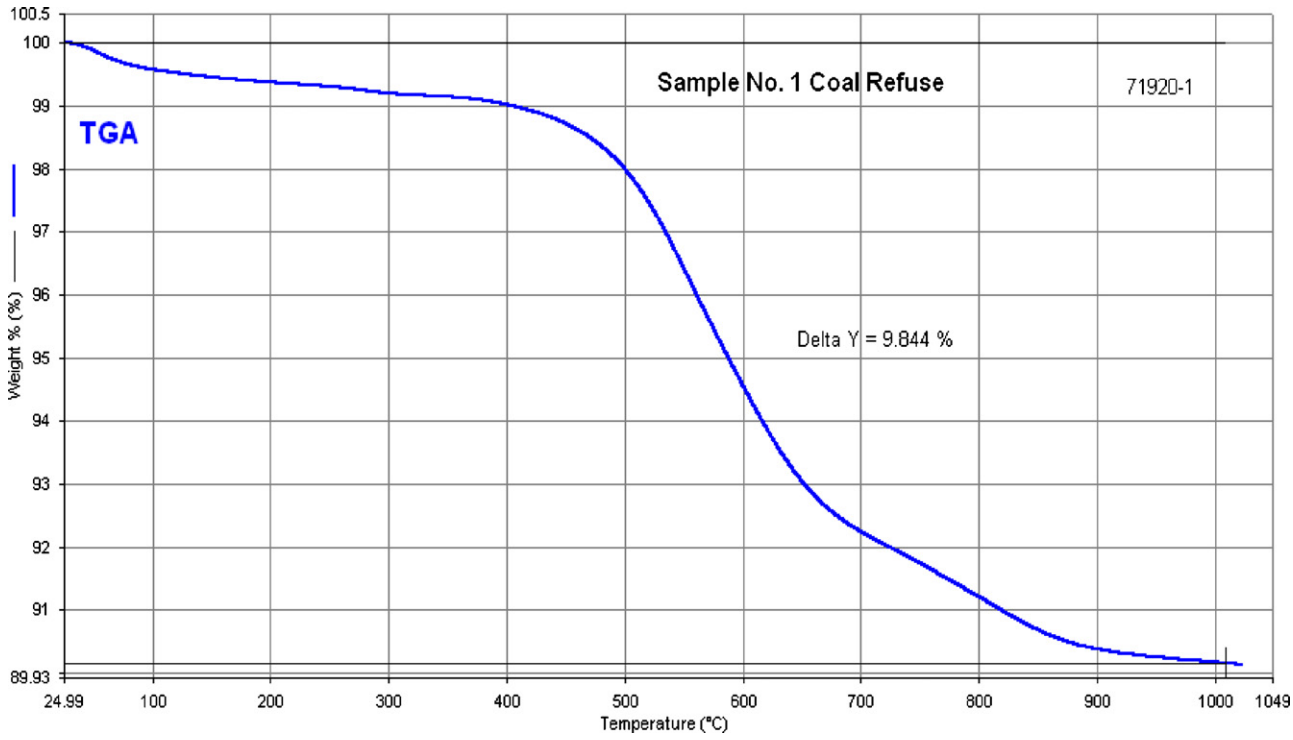

Fig. 7. TGA result for the coal refuse.

3.5.2. XRD and FTIR analysis

The mineral compositions of the activated material changed at different activation temperatures. Figs. 8 and 9 show the XRD results of the tabulated mineral compositions. It was found that the major minerals in the raw coal refuse were chlorite, muscovite, quartz, calcite, and kaolinite [24]. Quartz and mullite were the predominant minerals in the fly ash. Figs. 8 and 9 indicate that the change in the mineral phase of the coal refuse was significant, while the change for the fly ash was slight. These changes are summarized as follows:

1. The kaolinite peaks began to decrease because of their transformation into metakaolin at 550 °C, and the kaolinite peaks disappeared at 750 °C.
2. Chlorite peaks began decreasing at 550 °C and disappeared at 750 °C.
3. Muscovite peaks decreased at 750 °C and disappeared at 950 °C.
4. At 950 °C, the quartz peak was weakened by the thermal activation and may have been caused by the decomposition of clay minerals that formed amorphous silicon-based material.
5. The hematite peaks in XRD peaks becomes more evident after thermal activation, especially at 950 °C.
6. Calcite peaks decreased but still exist when the temperature rise up to 950 °C, which might due to the decomposition of the calcite [25].

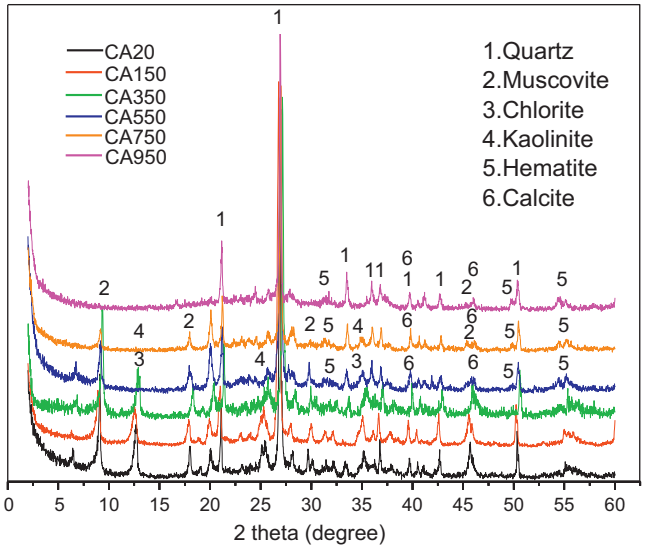

Fig. 8. XRD of the coal refuse at different activation temperatures.

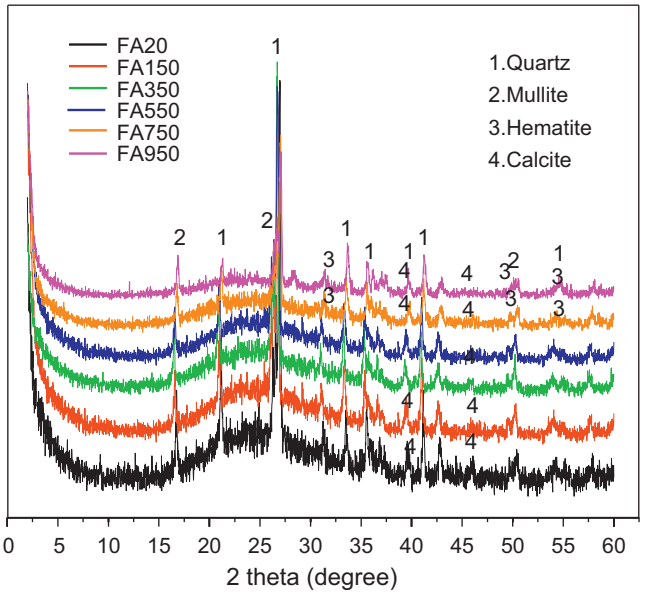

Fig. 9. XRD of fly ash at different activation temperatures.

Thermal activation of coal refuse can be considered to include calcinations at a certain temperature, after which kaolinite dewaters and decomposes, releases the hydroxide radical from Al—O octahedron, and changes the coordinate number of Al in kaolinite from 6 to 4 or 5 [26,32]. Metakaolin is a mineral with good pozzolanic material, which is generated during the thermal activation [27]. Previous studies have proved that the metakaolin can be obtained by the calcinations from 650 °C to 800 °C [28,29]. Brindley and Nakahira studied the phase transformation of kaolinite in the process of calcinations, and metakaolin was obtained at the temperature of 500 °C and transform to silicon-spinel at 925 °C and when the temperature is above 1400 °C, mullite is generated [30,31]. And it was noted that the silicon spinel and mullite both have low activity, and reaction can be generally expressed as the following [32].

$$\sim 500\,^{\circ}\mathrm{C}: \quad \underset{\text{(kaolinite)}}{Al_2O_3 \cdot 2SiO_2 \cdot 2H_2O} \rightarrow \underset{\text{(metakaolinite)}}{Al_2O_3 \cdot 2SiO_2} + 2H_2O$$

$$925\,^{\circ}\mathrm{C}: \quad 2[Al_2O_3 \cdot 2SiO_2] \rightarrow \underset{\text{(silicon-spinel)}}{2Al_2O_3 \cdot 3SiO_2} + SiO_2$$

$$1100\,^{\circ}\mathrm{C}: \quad 2Al_2O_3 \cdot 3SiO_2 \rightarrow \underset{\text{(1:1 mullite) type phase}}{2[Al_2O_3 \cdot SiO_2]} + SiO_2$$

$$> 1400\,^{\circ}\mathrm{C}: \quad 3[Al_2O_3 \cdot SiO_2] \rightarrow \underset{\text{(3:2 mullite) type phase}}{3Al_2O_3 \cdot 2SiO_2} + SiO_2$$

Therefore, in order to get better pozzolanic properties of the kaolinite by thermal activation, the temperature should be controlled under 925 °C.

At the same time, phase change also happen to the muscovite, which can be amorphized at high temperatures and high pressures [33]. Muscovite $2M_1$ has a major phase transition at approximately 800 °C, and the reaction occurring between 700 °C and 1000 °C is truly a dehydroxylation process, in which the muscovite $2M_1$ gradually dehydroxylates to muscovite HT [34]. This muscovite dehydroxylation occurs progressively through a non-homogeneous reaction process. The coordination change from 6 to 5 of Al atoms above 650 °C induces some structural changes, and the silicate layers are modified by the rotation of the tetrahedrons [35]. Thus, the progression of dehydroxylation helps to explain the increased pozzolanic properties of the coal refuse-based backfill material, as described above.

In addition, the decomposition of chlorite and decrease in the crystallinity of quartz happened during thermal activation, which also might explain the increased pozzolanic properties. That is because the previous studies show activated amorphous aluminosilicates have good pozzolanic properties, which are excellent for cementitious material development [36,37]. Furthermore, during thermal activation, hematite became more evident as the temperature rose from 20 °C to 950 °C. Calcite peaks decreased but still exist when temperature rise up to 950 °C, which might be due to decomposition of the calcite into lime and carbon dioxide. However, the ash carbonation is likely to occur when this thermal activation is exposed to air. Some portion of the lime from the calcite decomposition might react with the carbon dioxide. It is obvious that the thermal activation improves the pozzolanic properties of the coal refuse, but this process is a complicated physicochemical change which involves many aspects and further investigation is still required to discover the function of each specific phase change.

As for the XRD analysis of the fly ash, quartz, mullite, hematite and calcite are major four mineral phase. During the thermal activation, the hematite peaks were more evident while calcite peaks decreased but still exist as it did in the coal refuse. And a small quartz peak declined when the activation temperature was increased to 950 °C. This result indicated that these mineral phase

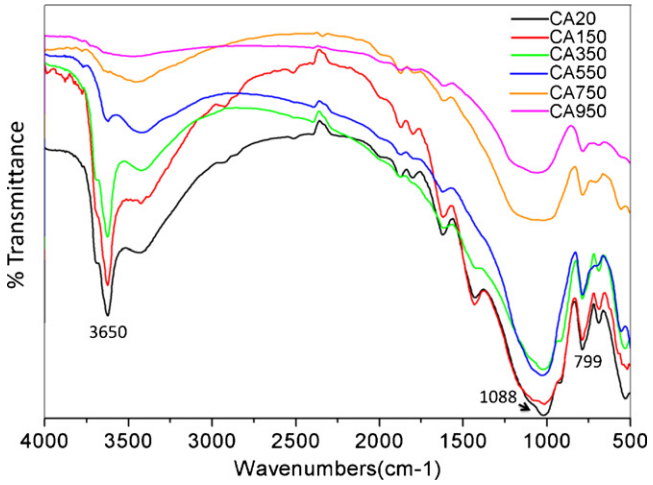

Fig. 10. FTIR spectra of the coal refuse at different activation temperatures.

changes might be attributed to the strength increase of the fly ash-based backfill material.

Figs. 10 and 11 represent the infrared spectra of thermal activated coal refuse and fly ash. In Fig. 10, the absorption at 1088 cm^{-1} is related to the anti-symmetric stretching mode of Si—O; the band at 799 cm^{-1} is attributed to the symmetric stretching vibration of Si—O—Si; and the bands at 1088 cm^{-1} and 799 cm^{-1} are indicative of quartz [36]. A sharp peak near 3650 cm^{-1} is associated with the O—H stretching vibrations in the muscovite and significantly declines when the temperature increases from 20 °C to 950 °C [38]. This result corresponds with the XRD results above and indicates that muscovite dehydroxylation occurs during the thermal activation of the coal refuse. However, in the infrared spectra of the fly ash, there is no significant absorption band shift during the thermal activation at different temperatures, although a slight absorption decline was observed near 3650 cm^{-1} and 1088 cm^{-1}.

3.5.3. SEM analysis

The SEM image in Figs. 12 and 13 illustrate the morphological characteristics of thermal-activated coal refuse and fly ash before milling. The reason for analyzing the coal refuse and fly ash before milling was to maintain the original morphological changes caused by different thermal activation conditions. Fig. 12(a)–(d) shows the "scale-shaped" layered structure; however, this structure was destroyed when the temperature reached higher than 750 °C. The

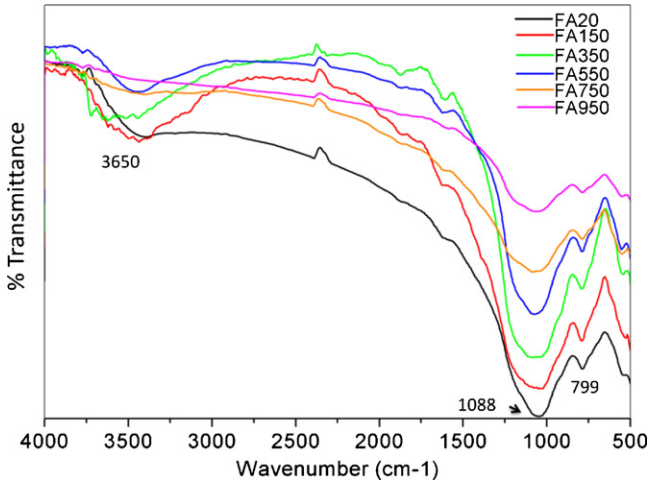

Fig. 11. FTIR spectra of the fly ash at different activation temperatures.

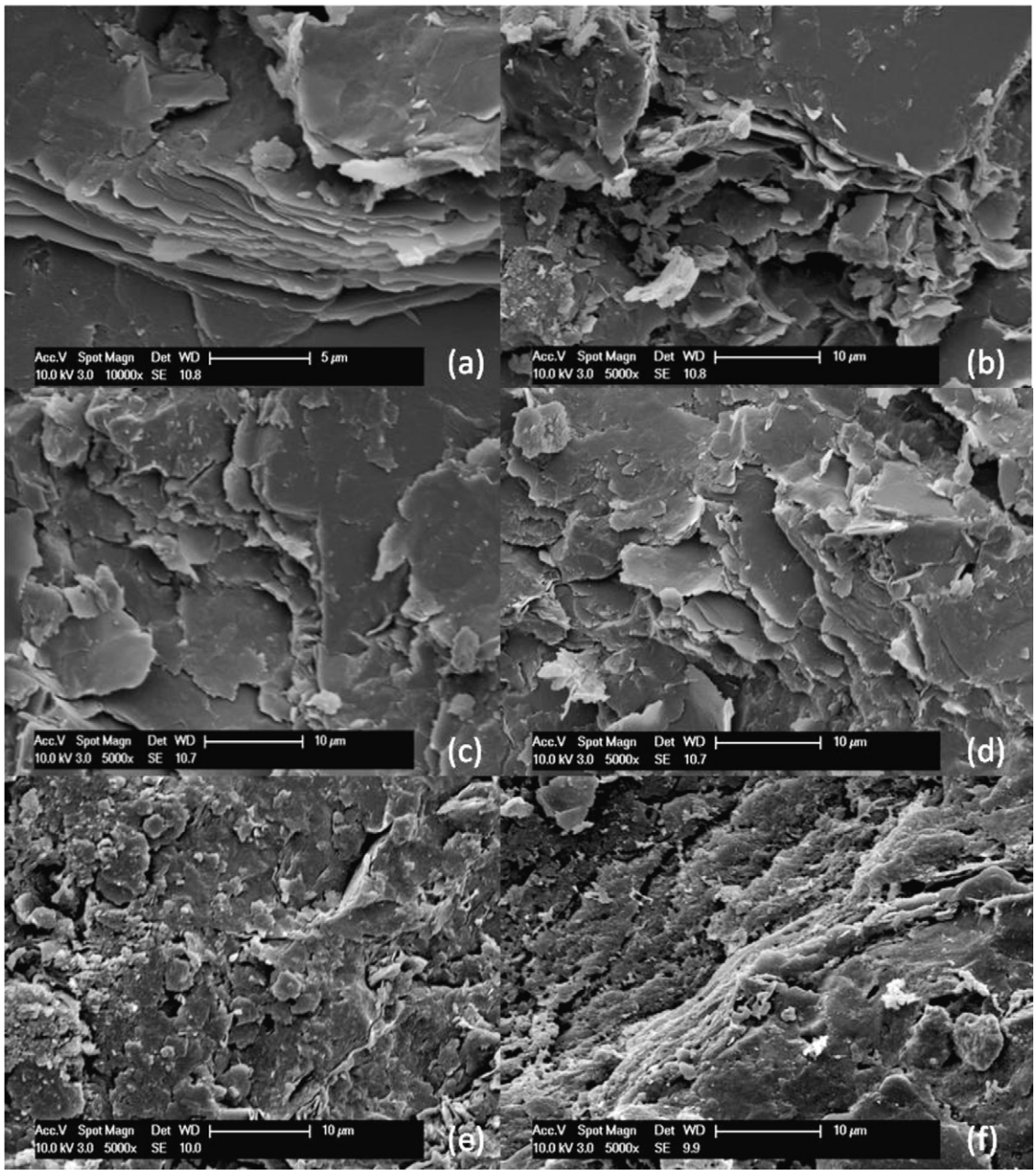

Fig. 12. SEM image of the coal refuse (after milling) activated at different temperatures: (a) 20 °C, (b) 150 °C, (c) 350 °C, (d) 550 °C, (e) 750 °C and (f) 950 °C.

decomposition of minerals, such as chlorite, muscovite, and kaolinite, may have caused the irregular and porous structure (Fig. 12(e) and (f)) because of the dehydroxylation and phase change of the minerals when the temperature was increased. The SEM images in Fig. 12 agree well with the XRD result shown in Fig. 8. Although the XRD result of the fly ash did not show much change when heated from 20 °C to 750 °C, the SEM image in Fig. 13 shows a significant morphological change in the fly ash. In Fig. 13(a)–(c), the fly ash is still a smooth and round spherical particle, with or without some small irregular particles adhering to the surface, whereas Fig. 13(d) indicates that some of the surface cover on the fly ash sphere began to crack when the temperature reached 550 °C. At 750 °C, similarly sized small particles relocated to the surface on the fly ash, as shown in Fig. 13(e). Fig. 13(f) shows an image of a fly ash sphere, covered with many small particles of relatively similar size, which may have come from the cracked exterior during thermal activation. This observation in Fig. 13 also explains the agglomeration phenomenon in the flowability test of the fly ash and fly ash-based backfill test. Therefore, the thermal activation process of fly ash from 20 °C to 750 °C showed a "Crack-Agglomeration" process, as described above.

Figs. 12 and 13 show the morphologic patterns of thermally activated coal refuse (before milling) and fly ash (before milling). Below 550 °C, most of the structure of the coal refuse was "scale-shaped" layered and became irregular and porous when the temperature was increased from 550 °C to 950 °C. The agglomeration phenomenon was obvious on the surface cover outside the fly ash sphere. These morphological changes were also observed for the coal refuse after milling and fly ash after milling, as shown in Fig. 14, although they are not as clear as those of the coal refuse and fly ash before milling because mechanical forces in the milling process destroyed their structure.

The microstructure of the B4 hardened backfill body was also investigated by SEM. Fig. 15 shows the different microstructure

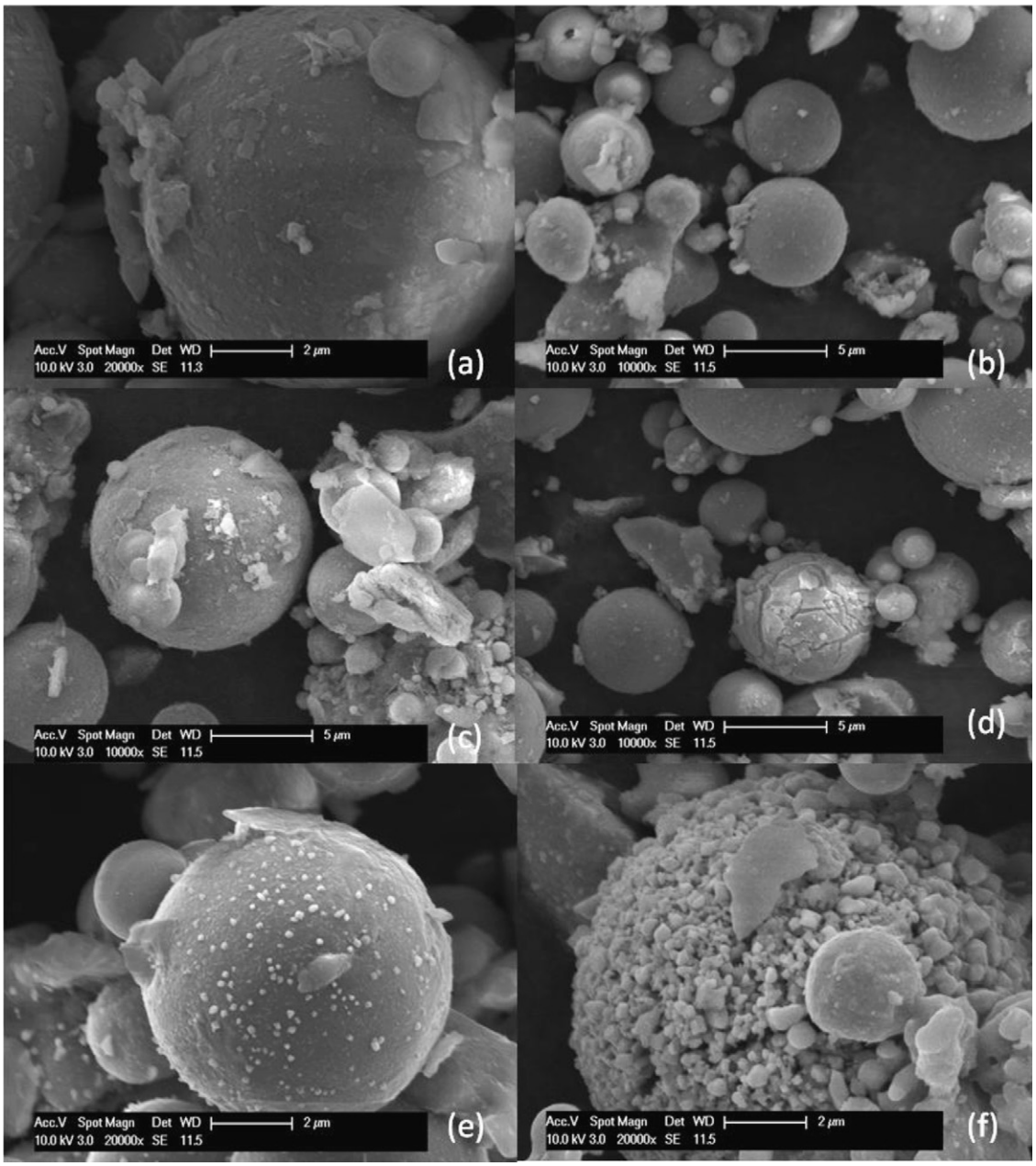

Fig. 13. SEM image of fly ash (after milling) activated at different temperatures: (a) 20 °C, (b) 150 °C, (c) 350 °C, (d) 550 °C, (e) 750 °C and (f) 950 °C.

characteristics. Fig. 15(a) and (b) shows the 3 day and 7 day microstructures of B4, which were composed of needle-shaped ettringite and rod-like $Ca(OH)_2$. However, the 28 and 90 day microstructures had a more amorphous gel outside the fly ash sphere and the matrix of the hardened backfill body. Some secondary formations of minerals are shown in Fig. 15(c) and (d), when the curing time reached 28 and 90 days.

3.6. TCLP results

Because backfill materials are rather permeable, the environmental effect of the material was also investigated, and the results are listed in Table 6. The main environmental concern surrounding the utilization of coal refuse, fly ash, and final products is the possibility that certain constituents will leach into the groundwater at concentrations determined to be potentially hazardous to human health [9]. However, the TCLP results of the raw fly ash, raw coal refuse and 180 day backfill hydration products B4 are shown in Table 6 and reveal that none of the metal leaching levels exceeded the EPA limitations. These results indicate that the backfill material is environmentally acceptable. There was also no significant difference in the leaching results between the raw coal refuse and the 750 °C activated coal refuse. Although some studies have been recently published on the relevant role of organic carbon on metal leaching [39–41], the total effect of organic carbon on metal leaching from the backfill material was not significant in this test. The mechanism of formation of organic carbon-heavy metal complexes and the related molecular modeling require further investigation.

3.7. Feasibility for current backfill industry

Backfill industry involves different factors which might influence the final application, such as backfill material, location of mine, geometry of the underground space, transportation facilities,

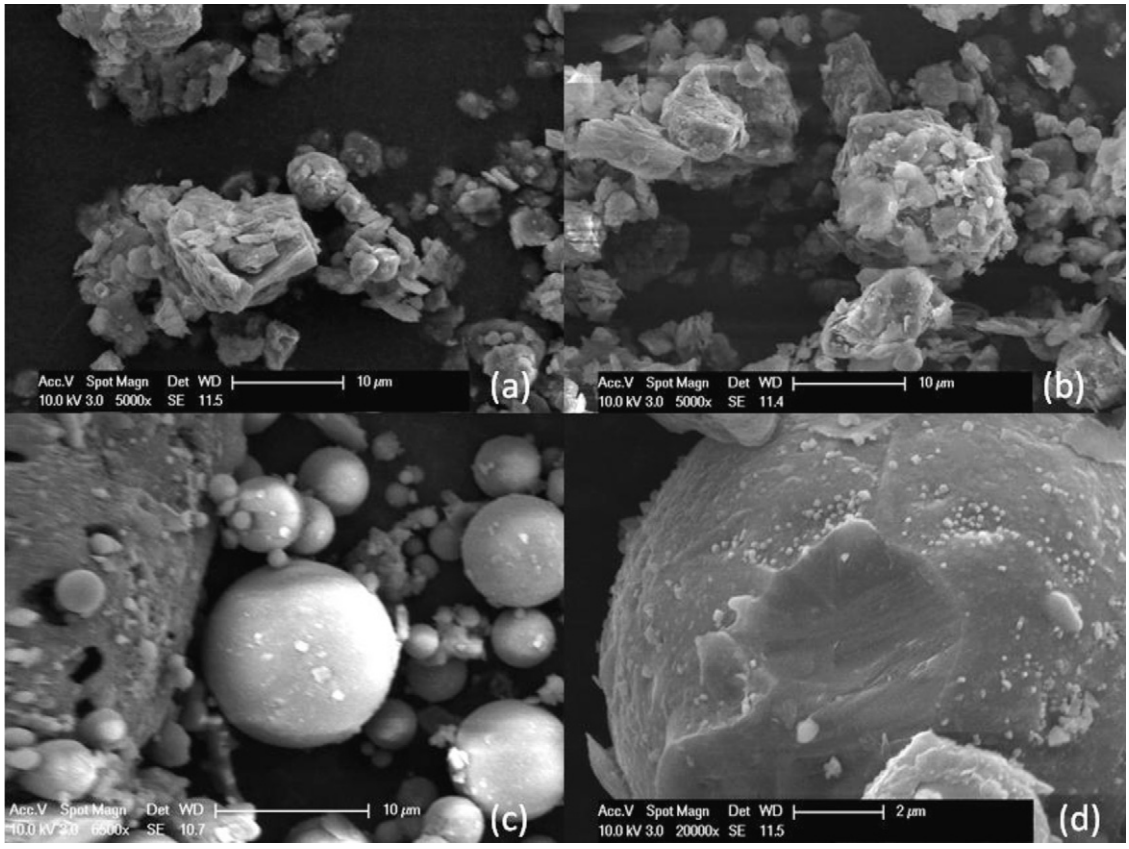

Fig. 14. SEM image of coal refuse (after milling) and fly ash (after milling) activated at 20 °C and 750 °C. (a) Coal refuse at 20 °C, (b) coal refuse at 750 °C, (c) fly ash at 20 °C and (d) fly ash at 750 °C.

etc. The performance and requirement of backfill material varies from mine to mine. According to Tony Grice from Australian mining consultants, there are currently three major backfill methods: hydraulic backfill, rock backfill and paste backfill [4]. Although each of these backfill methods has some unique characteristics, they still share some disadvantages when using largely Ordinary Portland cement as the binder. These disadvantages include the following: (1) a large amount of cement in the slurry is carried away by water during the dewatering process, which not only causes environmental problems but also decreases the strength of the backfill body. (2) Only the coarse fractions of the tailings can be used as aggregate to create high permeability in the backfill body. The utilization efficiency of the tailing is less than 40%. The large quantity of unused fine tailings must be disposed of, which causes environmental problems on mine surfaces. (3) The purchase of sands to create aggregates is costly if the amount of tailings available is not sufficient for backfill [6].

Alternatively, the introduced silica–alumina backfill material controls the pulp density of the backfill slurry at 70–75%, which provides high flowability and a low bleeding rate. This material uses mining waste-coal refuse as coarse aggregates and provides a huge economic benefit to industry. Along with 1% of cement, all materials used in this backfill technology are industrial waste resources, which means this backfill technology significantly reduces the cost of the industrial input. The major concern for this technology is energy and time input for the coal refuse thermal activation

Table 6
TCLP results.

Constituent	Raw fly ash (ppm)	Raw coal refuse (ppm)	750 coal refuse (ppm)	B4 180 day backfill sample (ppm)	EPA limits (ppm)
Antimony	0.37	<0.05	<0.05	<0.05	–
Arsenic	<0.05	<0.05	<0.05	<0.05	5.0
Barium	0.91	0.547	0.598	0.207	100.0
Beryllium	<0.025	<0.025	<0.025	<0.025	–
Cadmium	<0.025	<0.025	<0.025	<0.025	1.0
Chromium	0.15	<0.05	<0.05	<0.05	5.0
Cobalt	0.10	<0.01	0.0116	<0.01	–
Copper	<0.01	<0.01	0.0133	<0.01	–
Lead	<0.05	<0.05	<0.05	<0.05	5.0
Mercury	<0.0001	<0.0001	<0.0001	<0.0001	0.5
Molybdenum	<0.01	<0.01	<0.01	<0.01	–
Selenium	<0.01	<0.01	<0.01	<0.01	1.0
Silver	<0.05	<0.05	<0.05	<0.05	5.0
Thallium	<0.05	<0.05	<0.05	<0.05	–
Vanadium	<0.01	<0.01	<0.01	<0.01	–
Zinc	<0.01	<0.01	0.0242	<0.01	–

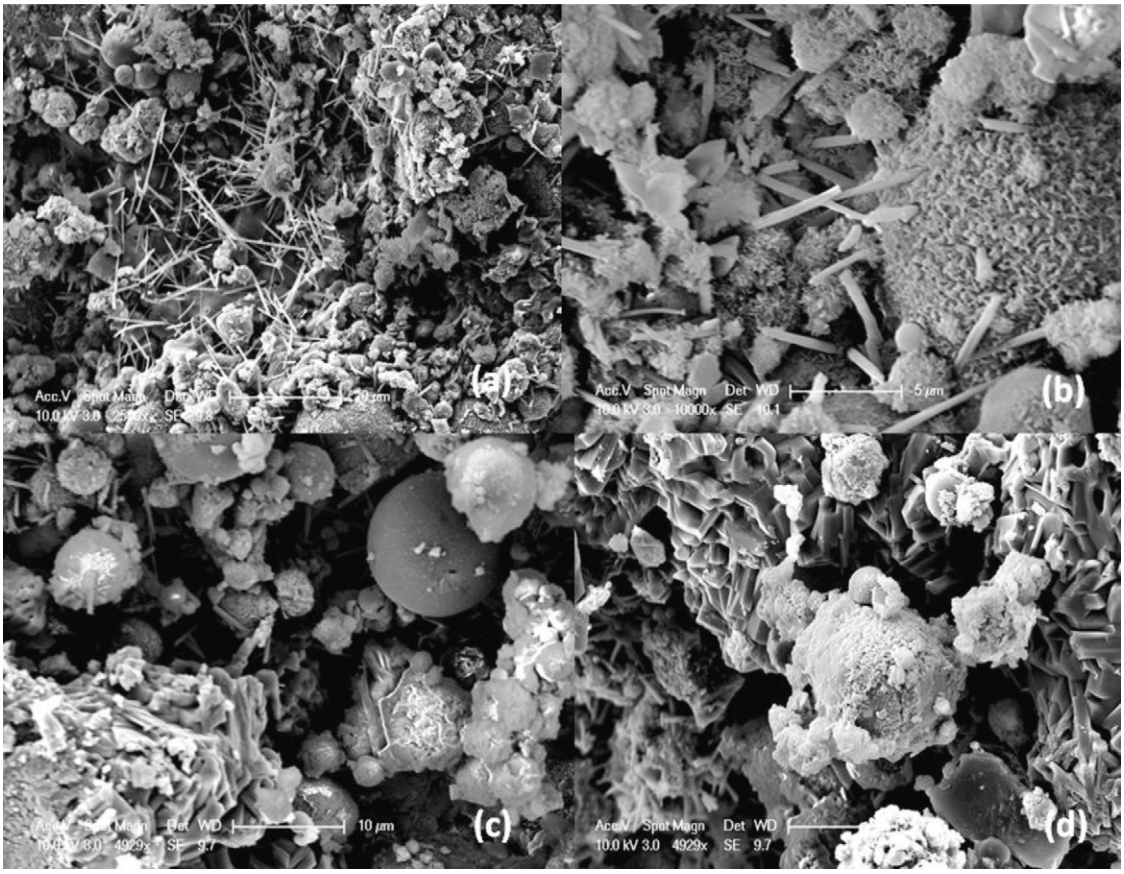

Fig. 15. SEM image of the hardened body of backfill material B4 at (a) 3 days, (b) 7 days, (c) 28 days and (d) 90 days.

Table 7
Technical index of the backfill technology.

Technical index	Hydraulic/rock backfill	Paste backfill	Silica alumina coal refuse based backfill
Binder	Cement	Cement	Cement, slag and gypsum
Aggregate	Coarse to medium course sand, rock	Graded tailings, total tailing, river sand	Coal refuse, fly ash, other industry wastes
Density	55–70%	75–85%	70–75%
Flowability	Good	Poor	Good
Transportation	By gravity	Using high pressure pump	By gravity or using low pressure pump
One-off investment	Relatively low	High	Relatively low
Filling capability	>100 m^3/h	30–50 m^3/h	>100 m^3/h
Processing	Complicated	Difficult	Relatively easy
Evaluation	Dewatering	No dewatering	No dewatering
	Low strength	Relative high strength	Relative high strength

process; however, the 45 min activation time is acceptable for backfill application. Additionally, thermal activated coal refuse accounts for only 5% of the total solid material, which means only a small amount of energy is consumed. Furthermore, the remainder of the thermal activated coal refuse is successfully used to produce coal refuse blended cement. In this case, the binary utilization of the thermal activated coal refuse makes this technology more realistic when considering economic factors. And Table 7 describes the advantages of this silica–alumina-based backfill material over the traditional backfill material.

4. Conclusions

The conclusions of the study are as follows:

(1) Coal refuse and fly ash have different pozzolanic properties when they are thermally activated from 20 °C to 750 °C. Coal refuse shows improvements in both pozzolanic properties and flowability. Although thermal activation slightly improves the pozzolanic properties of the fly ash, it decreases the flowability when the temperature increases from 550 °C to 950 °C because of a severe agglomeration phenomenon, as shown by the SEM images.
(2) B4 (5% 750 °C coal refuse + 15% 20 °C fly ash) presents the optimal design for this backfill material because of its excellent flowability and compressive strength and a low bleeding rate, which meets the requirements for a mining backfill.
(3) Microanalysis shows the mineral phase change of the coal refuse and fly ash during thermal activation. For the coal refuse, the kaolinite peaks begin to decrease because of kaolinite transformation to metakaolin at 550 °C, and chlorite peaks disappear at 750 °C. The muscovite peak decreases at 750 °C and totally disappears at 950 °C, during which muscovite $2M_1$ gradually dehydroxylates to muscovite HT. And the hematite peaks in

XRD result becomes more evident after thermal activation, especially at 950 °C. The fly ash did not show any significant mineral phase change during the thermal activation. This result agrees well with the SEM study on the microstructure of fly ash and coal refuse.

(4) Toxicity characteristic leaching procedure tests show that none of the tested elements in the hardened backfill body exceed the EPA limitations, indicating that the backfill material in this experiment is environmentally acceptable.

(5) In this silica–alumina backfill material, only 1% cement is introduced, the rest of the material is industrial solid waste, which offers enormous potential for reducing the capital investment for the backfill industry.

Acknowledgements

The author gratefully acknowledges the financial support from two organizations for this research work: the US Department of Energy (DOE-DE-EE0003496) and Pacific Resources Research Center.

References

[1] CTAB, International energy agency coal industry advisory board—32nd plenary meeting discussion report. OECD Headquarters in Paris, 2010.
[2] US EPA, Materials characterization paper in support of the advanced notice of proposed rulemaking: identification of nonhazardous materials that are solid waste-coal refuse, December 16, 2008.
[3] US EPA, Materials characterization paper in support of the final rulemaking: identification of nonhazardous materials that are solid waste-coal refuse, February 3, 2011.
[4] T. Grice, Underground mining with backfill, Australian mining consultants, in: The 2nd Annual Summit-Mine Tailing Disposal Systems, Brisbane, 1998, pp. 24–25.
[5] M. Benzaaoua, J. Ouellet, S. Servant, P. Newman, R. Verburg, Cementitious backfill with high sulfur content physical, chemical, and mineralogical characterization, Cement Concrete Res. 29 (5) (1999) 719–725.
[6] H. Sun, Y. Huang, B. Yang, The Contemporary Cemented Filling Technology, Metallurgical Industry Press, 2002 (in Chinese).
[7] R. Siddique, Utilization of waste materials and by-products in producing controlled low-strength materials, Resour. Conserv. Recycl. 54 (1) (2009) 1–8.
[8] S. Turkel, Strength properties of fly ash based controlled low strength material, J. Hazard. Mater. 47 (3) (2007) 1015–1019.
[9] S. Turkel, Long-term compressive strength and some other properties of controlled low strength materials made with pozzolanic cement and class C fly ash, J. Hazard. Mater. 137 (1) (2006) 261–266.
[10] A. Katz, K. Kovler, Utilization of industrial by-products for the production of controlled low strength materials (CLSM), Waste Manage. 4 (5) (2004) 501–512.
[11] B. Ercikdi, F. Cihangir, A. Kesimal, H. Deveci, I. Alp, Utilization of industrial waste products as pozzolanic material in cemented paste backfill of high sulphide mill tailings, J. Hazard. Mater. 168 (2–3) (2009) 848–856.
[12] N. Zhang, M. Liu, H. Sun, L. Li, Evaluation of blends bauxite-calcination-method red mud with other industrial wastes as a cementitious material: properties and hydration characteristics, J. Hazard. Mater. 185 (1) (2011) 329–335.
[13] N. Zhang, M. Liu, H. Sun, L. Li, Pozzolanic behaviour of compound-activated red mud–coal gangue mixture, Cement Concrete Res. 41 (3) (2011) 270–278.
[14] J. Zhang, H. Sun, Y. Sun, N. Zhang, Corrosion behavior of steel rebar in coal gangue based mortar, J. Zhejiang Univ. Sci. A 11 (5) (2011) 382–388.
[15] J. Zhang, H. Sun, Y. Sun, N. Zhang, Correlation between 29 Si polymerization and cementitious activity of coal gangue, J. Zhejiang Univ. Sci. A 10 (9) (2010) 1334–1340.
[16] J. Zhang, H. Sun, J. Wan, Z. Yi, Study on microstructure and mechanical property of inter-facial transition zone between limestone aggregate and sialite paste, Construct. Build. Mater. 23 (11) (2010) 3393–3397.
[17] ASTM C618-08, Standard Specification for Coal Fly Ash and Raw or Calcined Natural Pozzolan for Use in Concrete, American Society for Testing and Materials, Conshohocken, PA, USA, 2008.
[18] M.C. Nataraja, Y. Nalanda, Performance of industrial by-products in controlled low-strength materials (CLSM), Waste Manage 28 (7) (2008) 1168–1181.
[19] ASTM D6103-97, Standard Test Method for Flow Consistency of Controlled Low Strength Material (CLSM), American Society for Testing and Materials, Conshohocken, PA, USA, 1997.
[20] ASTM C232-07, Standard Test Methods for Bleeding of Concrete, American Society for Testing and Materials, Conshohocken, PA, USA, 2007.
[21] ACI 229R-99 Report, Controlled Low Strength Materials, American Concrete Institute, Farmington Hills, MI, USA, 1999.
[22] S. Zhou, Rate of pozzolanic reaction of two kinds of activated coal gangue, J. Shanghai Univ. 13 (4) (2009) 322–326.
[23] D. Li, Y. Chen, J. Shen, The influence of alkalinity on activation and microstructure of fly ash, Cement Concrete Res. 30 (6) (2000) 881–886.
[24] X. Song, J. Han, Z. Gao, Effect of added-calcium thermal activated coal gangue on cement hydration, Adv. Mater. Res. 71–78 (2011) 833–836.
[25] C. Zhang, X. Yang, Y. Li, Mechanism and structural analysis of the thermal activation of coal-gangue, Adv. Mater. Res. 356–360 (2012) 1807–1812.
[26] S. Lee, Y. Kim, H. Moon, Energy-filtering transmission electron microscopy (EFTEM) study of a modulated structure in metakaolinite, represented by a 14 A modulation, J. Am. Ceram. Soc. 86 (2003) 174–176.
[27] A. Caldaron, R. Burg, High-reactivity metakaolin: a new generation material, Concrete Int. 11 (1994) 37–40.
[28] J. Ambroise, M. Murat, J. Pera, Hydration reaction and hardening of calcined clays and related minerals. V. Extension of the research and general conclusion, Cement Concrete Res. 15 (2) (1985) 261–268.
[29] J. Pera, Metakaolin and calcined clays, Cement Concrete Compos. 23 (6) (2001) iii.
[30] G. Brindley, M. Nakahira, A new concept of the transformation sequence of kaolinite to mullite, Nature 181 (1958) 1333–1334.
[31] G. Brindley, M. Nakahira, The kaolinite–mullite reaction series. IV. The coordination of aluminum, J. Am. Ceram. Soc. 44 (10) (1961) 506–507.
[32] C. Li, H. Sun, L. Li, A review: the comparison between alkali-activated slag (Si + Ca) and metakaolin (Si + Al) cements, Cement Concrete Res. 40 (9) (2010) 1341–1349.
[33] P. Zanazzi, A. Pavese, Behavior of micas at high pressure and high temperature, Rev. Miner. Geochem. 6 (1) (2002) 99–106.
[34] E. Mazzucato, G. Artioli, A. Gualtieri, High temperature dehydroxylation of muscovite-$2M_1$: a kinetic study by in situ XRPD, Phys. Chem. Miner. 6 (5) (1999) 375–381.
[35] F. Gridi-Bennadji, B. Beneu, J.P. Laval, P. Blanchart, Structural transformations of muscovite at high temperature by X-ray and neutron diffraction, Appl. Clay Sci. 38 (3–4) (2008) 259–267.
[36] C. Li, J. Wan, H. Sun, L. Li, Investigation on the activation of coal gangue by a new compound method, J. Hazard. Mater. 179 (1–3) (2010) 515–520.
[37] N. Zhang, H. Sun, X. Liu, J. Zhang, Early-age characteristics of red-mud–coal gangue cementitious material, J. Hazard. Mater. 167 (1–3) (2009) 927–932.
[38] M. Zhang, S. Redfern, E. Salje, M. Carpenter, L. Wang, H_2O and the dehydroxylation of phyllosilicates: an infrared spectroscopic study, Am. Miner. 95 (11–12) (2010) 1686–1693.
[39] P. Schwab, D. Zhu, M. Banks, Heavy metal leaching from mine tailings as affected by organic amendments, Bioresour. Technol. 98 (15) (2007) 2935–2941.
[40] R. Ludwig, R. McGregar, D. Blowes, S. Benner, K. Mountjoy, A permeable reactive barrier for treatment of heavy metals, Ground Water 40 (1) (2002) 59–66.
[41] S. Brown, C. Henry, R. Chaney, H. Compton, P.S. DeVolder, Using municipal biosolids in combination with other residuals to restore metal-contaminated mining areas, Plant Soil 49 (1) (2003) 203–215.